Chromatic confocal metalens and scattering medium-based speckle pattern engineering for compact, low-cost distometers

Przemyslaw Falak,[1,*] Justin Ho-Tin Chan,[2] James Williamson,[2] Andrew Henning,[2] Haydn Martin,[2] Xiangqian Jiang,[2] Shahrzad Zahertar, [1] Bruno Moog, [1] Timothy Lee,[1] Christopher Holmes,[1] Gilberto Brambilla,[1] and Martynas Beresna[1]

[1] *Optoelectronics Research Centre, University of Southampton, University Road, Southampton, SO17 1BJ, United Kingdom*

[2] *Centre for Precision Technologies, University of Huddersfield, Queensgate, Huddersfield, HD1 3DH, United Kingdom*

[*] *p.falak@soton.ac.uk*

Abstract: We demonstrate a reconstructive distometer with 0.78 micron resolution and 2.5 cm cubic footprint, utilising an engineered metalens and laser-written scattering medium for tailored speckle pattern generation, benefiting from low-cost, compact size and high stability.

1. Introduction

Developing low-cost and compact metrology devices is always welcomed by industry due to ever increasing requirements for sensing technology, including size, resolution, price and stability. In this paper, a chromatic confocal metalens and scattering medium-based wavemeter were demonstrated in tandem to realise a simple, low-cost and compact distance meter (distometer). The operating principle is based on two phenomena: (1) for a given wavelength there is only one specific focal distance for the same lens (chromatic confocal probe) [1, 2] and (2) in the scattering medium, light of a given wavelength is converted (mapped) into a unique and deterministic 2D speckle pattern, depending on the polarisation state and wavelength [3]. Therefore, for a surface at a given distance from the metalens, only one wavelength will be in focus and it can be mapped to its 2D speckle pattern. Repeating this over the span of the distances for the whole confocal metalens range, the collection of speckles can be used as a calibration set with which measurement of an unknown position can be realised by applying singular value decomposition (SVD) [4–6].

2. Experiment Details

2.1. Setup

Figure 1(a) shows the layout, with a fiberised broadband source (450-2000 nm, 60 mW, WhiteLase micro, Fianium) launched into 50:50 coupler/splitter. One output port is directed to the the metalens which is fixed in place. The plane mirror was mounted on a translation stage (MTS25-Z8, Thorlabs) and placed approximately 1 mm from the metalens. The backreflected light returns via the coupler into the flat-fibre scattering medium-based sensor (Fig. 1(b)) for speckle pattern generation and capture by camera.

2.2. Metalens probe

A chromatic confocal probe uses the depth sectioning effect of a confocal microscope combined with a wavelength dependent focal position to determine an object's location from the wavelength most strongly returned. The advantage of using a metalens is the high degree of chromatic aberration that leads to a strongly wavelength dependant focal position without additional elements. An optical fibre acts as both the point source and point detector, and thus the entire probing side of the instrument is created from just two elements. The mechanism by which the location of the scattering object changes the signal detected is illustrated in Fig. 2(a). The metasurface (*MS*), focuses different wavelengths to different points longitudinally, and after reflection from the mirror (*M*) the light once again passes through the metasurface. Only light in focus around the mirror is refocused onto the end of the fibre (*F*), with light focused before or after the mirror being spread out at the end of the fibre, thus coupling less power back towards the detector. By measuring which wavelengths are focused onto the end of the fibre, the wavelengths that were focused onto the surface, and hence the location of the object after the metasurface, is determined. The metalens is constructed by etching a square array of 750 nm high pillars, with centre to centre

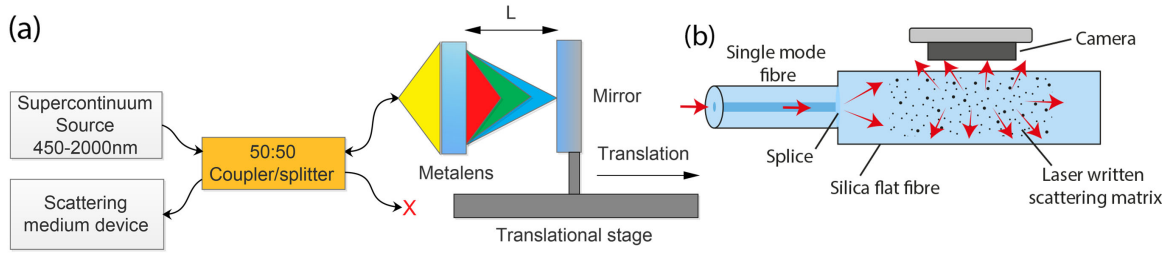

Fig. 1. (a) Experimental layout for distometer. Broadband supercontinuum source is connected to 50:50 coupler and projected onto metalens. The wavelength whose focal distance matches the distance L to the mirror is reflected back into the coupler to reach (b) the scattering medium-based device which scatters the light into a speckle pattern to be imaged by the camera.

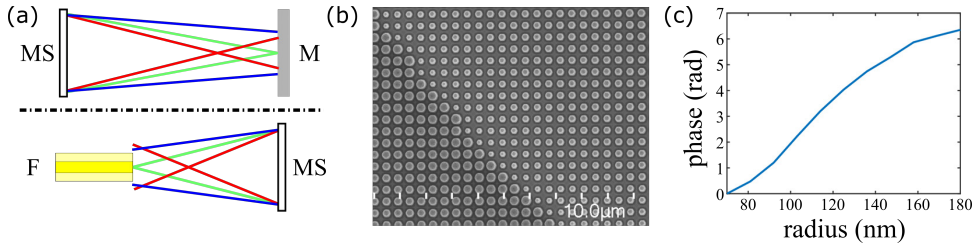

Fig. 2. (a) Effect of mirror location (M) on signal detected. Upper: wavelength dependant focal spot after the metasurface (MS). Lower: collection of the scattered light by the fibre (F). (b) SEM image of metasurface. (c) Phase delay of light passing through metasurface against pillar radius.

distance of 450 nm, from the surface of a 4.5 μm layer of GaN on a 430 μm thick wafer of Al_2O_3, as shown in Fig. 2(b). The phase delay is varied by up to 2π radians across the surface by changing the pillar radii from 70 nm to 180 nm. In this way, any arbitrary incident wavefront can be converted into an arbitrary output wavefront (modulo 2π). In order to focus the light at a distance f along the optical axis, its phase after the metasurface needs to be:

$$\phi_{out}(x,y) = -\frac{2\pi}{\lambda}(\sqrt{x^2+y^2+f^2} - f) \tag{1}$$

where λ is the wavelength of the light, $\phi_{out}(x,y)$ is the phase of the light, and the top surface of the metasurface lies in the plane $z = 0$. The phase of the incident light across the base of metasurface needs to be known in order to calculate the phase delay that is needed to produce the phase given by Eqn. 1 after it. The end of the fibre (Thorlabs, P3-630A-FC-2) will be considered to be a point source which lies a distance $z_{fibre} = 7$ mm before the base of the substrate, allowing the cone of light to expand sufficiently to cover the entire 1×1 mm area of the metasurface. If the substrate was not present, the phase of the incident light would be equal to that given by Eqn. 1 only with the distance f being replaced by the distance from the fibre to the metasurface. Ignoring the substrate would however lead to spherical aberration being present, and so ray tracing is used to take into account the refraction at the surface and find the optical path length from the center of the optical fibre to the center of each of the pillars on the metasurface, and from this the phase of the incident light at the base of the metasurface $\phi_{in}(x,y)$. The relative phase delay that the metasurface needs to impart at a point (x,y) is therefore $\phi_{out}(x,y) + \phi_{in}(x,y)$.

Both Eqn. 1 and the phase delay that the pillars impart are wavelength dependant, and so will only be satisfied at the design wavelength ($\lambda = 660$ nm). For longer wavelengths, the curvature of the wavefront after the metasurface is greater than that given by Eqn. 1, focusing the light closer to the metasurface than f = 1 mm, while for shorter wavelengths the curvature is less than that given by Eqn. 1 focusing the light to a point beyond f = 1 mm.

2.3. Speckle generation and distance reconstruction

Once the light is reflected at the given distance from the metalens, it needs to be converted to the speckle pattern for further processing. To achieve this, an engineered array of scattering centres has been developed via laser-writing [3,7]. The speckle pattern is a 2D plane projection of the light after multiple interference from the scattering centres. In principle, the scattering changes the propagation direction of light, so realizing multiple scatterer arrays enhances the randomization of the optical path and as a result lengthens the average optical path [8]. This in turn enables high spectral resolution.

The scattering matrix was inscribed in fused silica flat fiber by femtosecond laser-writing system (Pharos, Light Conversion, λ=515 nm) [3]. The use of a flat fibre substrate, rather than circular fibre, eliminated challenges related to the stability of the device and improved insensitivity to the environmental fluctuations (geometric rigidity and compactness of the device) during the measurement process. The fully-assembled device measures only $2.5 \times 2.5 \times 2.5$ cm.

To reconstruct the measurand (distance L) from the speckles collection, each speckle image is converted to grayscale values as 2D matrices and then vectorized as a single-column matrix. The value recovery is based on the two speckles sets: (1) the calibration for known measurand and (2) test dataset with 'unknown' value within the calibration range [4]. The vectorized calibration speckles are further processed to form calibration matrix C by appending each consecutive speckle from calibration set as the neighbouring column of the newly-formed matrix. Multiplying the unknown speckle vector P from the test set with the inverse of the calibration matrix C^{-1} results in the correlation vector W, which shows the correlation number of how much of each speckle vector from the calibration pattern is constituting the unknown vector and the calibration speckle which corresponds to the highest value of the correlation is presumed to match the tested value and the measurand is recovered (Eqn. 2) [5, 9, 10].

$$W = C^{-1} \cdot P \tag{2}$$

Since the simple inverse of the non-square matrix does not exist, the Moore-Penrose pseudo-inverse is instead computed, by singular value decomposition, which guarantees computational simplification and low inversion noise generation which may affect the reconstruction results.

3. Results and Discussion

The experiment was divided into two parts: (1) confocal measurement with CCS100 spectrometer as a reference, and (2) full-scale distometer operation based on the confocal measurement and speckle pattern measurements.

The reference measurement was done by replacing the scattering medium-based detector with the CCS100 spectrometer (Thorlabs). The mirror was then moved further away from the metalens over the range 1.34-1.52 mm in 0.02 mm steps. For each mirror position, the 620-740 nm spectrum was captured (Fig. 3). The results indeed confirm the peak position is linearly blue-shifting as the distance from the metalens increases. Whilst the peak position is important, the spectral shape impact cannot be omitted: the greater the separation distance is, the spectra become out-of-shape and had a wider bandwidths.

Full-scale measurements of the distometer were done by displacing the mirror over the distance range 1.50-1.52 mm in 0.03 μm steps, which corresponds to 1 encoder count of the translation stage. The dataset was acquired twice at the same conditions - once for calibration purposes and a repeat set for testing. Recalling the spectral measurements, the input light was expected to have a well-defined peak but lower intensity. Similarly, reconstruction was possible with SVD and the results indeed confirm the distometer with 0.78 μm standard error can be realised (Fig. 4(e)). An important part of this research was to establish the rationale behind the limiting performance of the device: the standard error of 0.78 microns was far greater than the minimal translation distance of 0.03 microns. The most probable is that over the given distance range, the spectral shape is not consistent - instead both the peak intensity and bandwidth vary, more prominently for the greater distances from the metalens (Fig. 4(a-d)). Indeed, well-defined speckle patterns can only be obtained for narrowband and high signal-to-noise

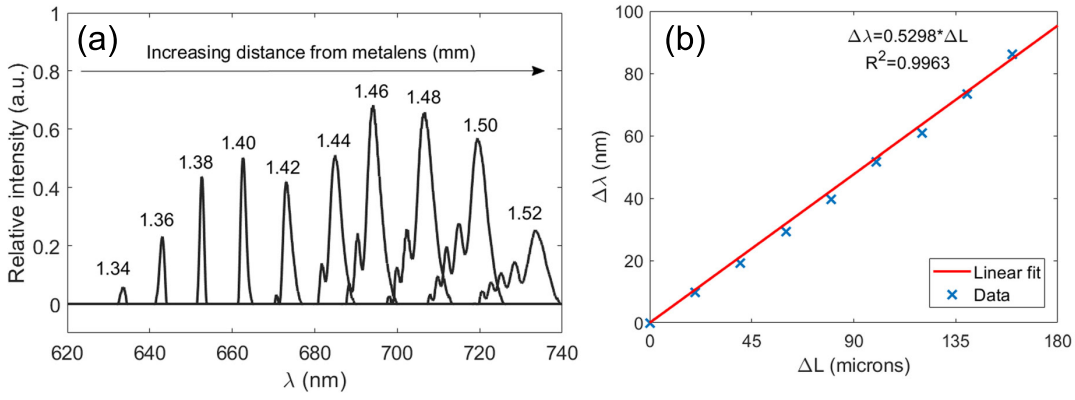

Fig. 3. (a) Reflected light spectra for different distances between metalens and mirror (distance in mm indicated above peaks). (b) Linearity of wavelength shift $\Delta\lambda$ against displacement distance ΔL.

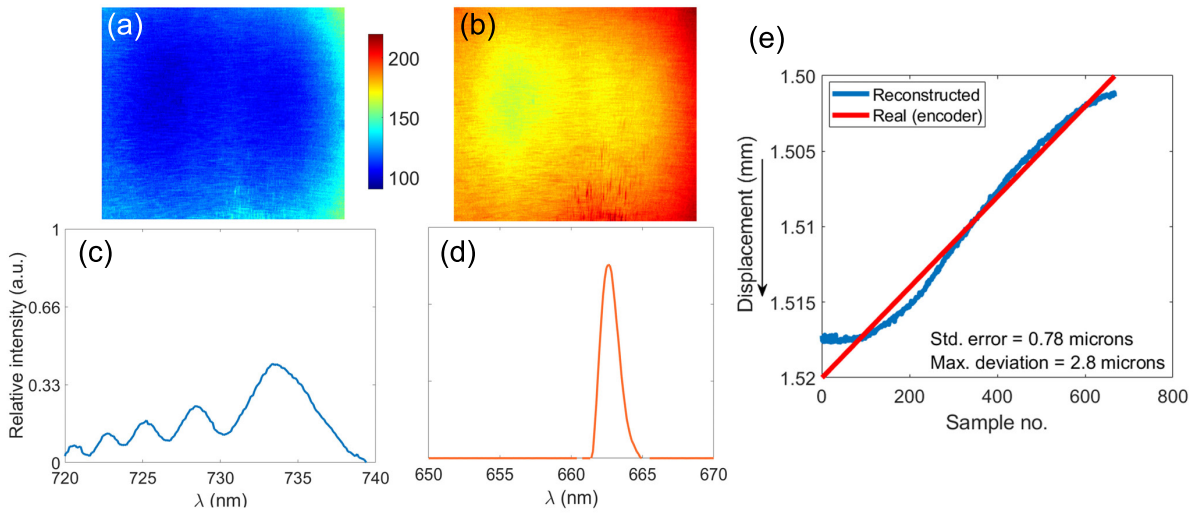

Fig. 4. (a, c) Low dynamic range speckle pattern, due to broadband input, and (b, d) well-defined speckle pattern with characteristic motifs, from narrowband input. Colourbar corresponds to 8-bit pixel value (0-255). (e) Reconstructed mirror displacement measurement. Red line indicates true reference position and blue line the values reconstructed from speckle measurement.

ratio input light. One shall expect the reconstruction for the greater separation distance to deviate more from the reference value and this indeed can be confirmed from the obtained results (Fig. 4(e)).

4. Conclusions

The application of an engineered metalens surface and scattering medium-based speckle detector in tandem realised the potential of a compact and low cost distometer with 0.78 micron resolution, by merging together chromatic confocal sensing with speckle pattern-based image analysis and quantity reconstruction. It also demonstrated the importance of the reflected light spectrum - the peak intensity and its bandwidth - on the generated speckle and the reconstructed measurand. Such a system has the potential to be further developed for 2D surface profiling and scanning.

References

1. F. Blateyron, "Chromatic confocal microscopy," in *Optical Measurement of Surface Topography,* R. Leach, ed. (Springer Berlin Heidelberg, Berlin, Heidelberg, 2011), pp. 71–106.
2. J. Chan, D. Tang, J. Williamson, H. Martin, A. Henning, and X. Jiang, "An ultra-compact metasurface-based chromatic confocal sensor," CIRP Ann. (2023).
3. Q. Sun, P. Falak, T. Vettenburg, T. Lee, D. B. Phillips, G. Brambilla, and M. Beresna, "Compact nano-void spectrometer based on a stable engineered scattering system," Photon. Res. **10**, 2328–2336 (2022).
4. B. Redding, S. F. Liew, R. Sarma, and H. Cao, "Compact spectrometer based on a disordered photonic chip," Nat. Photonics **7**, 746–751 (2013).
5. S. Brunton and J. Kutz, "Singular value decomposition (SVD)," in *Data-driven Science and Engineering: Machine Learning, Dynamical Systems, and Control,* (Cambridge University Press, 2019), pp. 3–46.
6. L. Devaud, B. Rauer, J. Melchard, M. Kühmayer, S. Rotter, and S. Gigan, "Speckle engineering through singular value decomposition of the transmission matrix," Phys. Rev. Lett. **127**, 093903 (2021).
7. P. L. Falak, Q. Sun, T. Vettenburg, T. Lee, D. B. Phillips, G. Brambilla, and M. Beresna, "Femtosecond laser written scattering chip for high-resolution low-cost reconstructive spectrometry," in *Photonic Instrumentation Engineering IX,* vol. 12008 (SPIE, 2022), p. 120080E.
8. B. Redding, S. F. Liew, R. Sarma, and H. Cao, "On-chip random spectrometer," in *Applied Industrial Optics: Spectroscopy, Imaging and Metrology,* (Optical Society of America, 2014), pp. AM2A–4.
9. S. L. Brunton, J. N. Kutz, X. Fu, and M. Johnson, "Data driven control of complex optical systems," in *Nonlinear Optics,* (Optica Publishing Group, 2015), p. NW4A.41.
10. J. Yang and J. yu Yang, "From image vector to matrix: a straightforward image projection technique—IMPCA vs. PCA," Pattern Recognit. **35**, 1997–1999 (2002).